International Tables for X-ray Crystallography (1974). Vol. IV. Birmingham: Kynoch Press.

JACK, A., LADNER, L. & KLUG, A. (1976). *J. Mol. Biol.* **108**, 619–649.

JOHNSON, C. K. (1965). *ORTEP*. Report ORNL-3794. Oak Ridge National Laboratory, Tennessee.

MAIN, P., HULL, S. E., LESSINGER, L., GERMAIN, G., DECLERCQ, J.-P. & WOOLFSON, M. M. (1978). *MULTAN 78. A System of Computer Programs for the Automatic Solution of Crystal Structures from X-ray Diffraction Data*. Univs. of York, England, and Louvain, Belgium.

TANAKA, K., FUJII, S., FUJIWARA, T. & TOMITA, K. (1979). *Acta Cryst.* B**35**, 929–933.

UESUGI, S., YASUMOTO, M., IKEHARA, M., FANG, K. N. & Ts'o, P. O. P. (1972). *J. Am. Chem. Soc.* **94**, 5480–5486.

UNICS (1973). *The Universal Crystallographic Computing System*. Library of Programs, Computation Center, Osaka Univ.

WANG, A. H.-J., QUIGLEY, G. J., KOLPAK, F. J., VAN DER MAREL, G., VAN BOOM, J. H. & RICH, A. (1981). *Science*, **211**, 171–176.

Acta Cryst. (1982). B**38**, 570–575

X-ray Structure and Crystal Packing Analysis of Triphenylchloromethane*

BY A. DUNAND AND R. GERDIL†

Département de Chimie Organique et Laboratoire de Radiocristallographie, Université de Genève, 30 quai Ernest Ansermet, 1211 Genève, Switzerland

(*Received* 8 *July* 1981; *accepted* 5 *August* 1981)

Abstract

$C_{19}H_{15}Cl$ is trigonal, space group $P\bar{3}$, with a = 13·998 (2), c = 13·202 (4) Å, V = 2240·2 Å^3, Z = 6, D_m = 1·26, D_x = 1·240 Mg m^{-3}, $F(000)$ = 876, μ = 0·225 mm^{-1}. The final R and R_w, based on 905 reflections, are 0·038 and 0·025 respectively. The molecules lie in special positions on the crystallographic threefold axes. They are associated in pairs and form two distinct $Ph_3C-Cl\cdots Cl-CPh_3$ head-to-head arrangements characterized by long C—Cl bonds and short Cl···Cl contacts. The shortest Cl···Cl distance (3·210 Å) is about 0·3 Å smaller than the sum of the van der Waals radii. For the sake of comparison, the lattice energy was computed using two different sets of Buckingham potential functions. The effects of including electrostatic terms were also investigated. These calculations account satisfactorily for all the salient features of the crystal packing. Analysis of the thermal motion showed that the rigid-body approximation holds reasonably well for the triphenylchloromethane molecule.

* (Chloro)triphenylmethane.

†To whom correspondence should be addressed.

0567-7408/82/020570-06$01.00

Introduction

Triphenylchloromethane (TPCM) was first described by Hemilian (1874). The continuous interest in its molecular conformation goes back to the early chemistry of free radicals (Gomberg, 1900). Young (1931) measured the cell parameters for the triclinic and trigonal forms. Wang & Lu (1944) examined the isomorphous trigonal forms of TPCM and triphenylbromomethane and concluded that these molecules lie in special positions on the crystallographic threefold axes. Further studies by Landais (1953) and Stora & Poyer (1966) revealed the presence of short Br···Br intermolecular contacts in triphenylbromomethane crystals. Spurred on by these preliminary accounts we have carried out the structure analyses of TPCM and triphenylbromomethane (Dunand & Gerdil, 1981) to obtain comparative information on short halogen–halogen interactions (Dunand, 1977; Dunand & Gerdil, 1976*b*). Both structures display linear $C-X\cdots X-C$ arrangements with long $C-X$ bonds and unusually short $X\cdots X$ contacts. The influence of the crystallization conditions on the formation of trigonal and/or triclinic TPCM crystals, as well as the geometrical relationship between the respective lattices,

© 1982 International Union of Crystallography

have been described elsewhere (Gerdil & Dunand, 1975).

Experimental

Colourless hexagonal prisms were grown from dry petroleum ether containing 0·5% acetyl chloride. The crystals are hygroscopic and were sealed under argon in Lindemann capillaries. The lattice parameters and the intensities were measured at room temperature on a four-circle Philips PW1100 diffractometer (graphite monochromator, Mo $K\alpha$ radiation).

With a crystal of dimensions 0·40 × 0·40 × 0·60 mm 1380 independent reflections were scanned in the ω–2θ mode (scan width 1°; scan speed 0·02° s^{-1}) within the range $2{\cdot}6° \leq \theta \leq 20{\cdot}0°$. After the usual corrections (absorption corrections were neglected) 905 reflections were considered observed at the $2\sigma(I)$ level and used in the structure analysis. The structure was solved by the heavy-atom method. All the H atoms were located from a difference synthesis. Positional and anisotropic thermal parameters for the Cl and C atoms (the H atoms were included with isotropic temperature factors) were refined by full-matrix least-squares analysis. The function minimized was $\sum w\Delta F^2$, where $w = 1/(0{\cdot}43 - 0{\cdot}00255F_o)^2$. The final R and R_w values were 0·034 and 0·025 respectively. Calculations were performed with the XRAY system (1972). The numbering system is shown in Fig. 1. The final atomic parameters are listed in Table 1.*

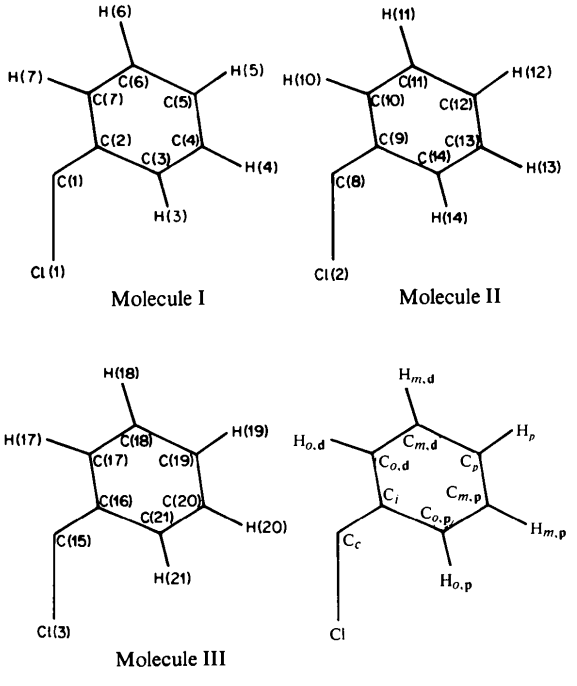

Fig. 1. The atom-numbering system and labelling scheme. i = *ipso*, o = *ortho*, m = *meta*, p = *para*; **p** = proximal, **d** = distal.

Table 1. *Fractional coordinates* ($\times 10^4$) *and thermal parameters* ($\times 10^3$)

Thermal parameters are given in the form

$$U_{eq}\,(\text{Å}^2) = \tfrac{1}{3}\sum_i \sum_j U_{ij}\, a_i^*\, a_j^*\, \mathbf{a}_i.\mathbf{a}_j.$$

	x	y	z	U_{eq}/U_{iso}
Cl(1)	0	0	1357 (1)	111 (1)
C(1)	0	0	2777 (4)	74 (3)
C(2)	1183 (3)	817 (4)	3099 (3)	72 (2)
C(3)	1731 (5)	1895 (5)	2714 (3)	93 (3)
C(4)	2780 (5)	2646 (4)	3056 (4)	108 (3)
C(5)	3299 (4)	2353 (5)	3769 (4)	103 (3)
C(6)	2775 (4)	1306 (5)	4145 (3)	91 (3)
C(7)	1721 (4)	540 (4)	3814 (3)	77 (3)
Cl(2)	6667	3333	2420 (1)	114 (1)
C(8)	6667	3333	1021 (4)	68 (3)
C(9)	5528 (4)	2419 (3)	702 (3)	71 (2)
C(10)	5399 (4)	1686 (4)	−59 (3)	80 (3)
C(11)	4357 (5)	880 (4)	−384 (3)	98 (3)
C(12)	3442 (5)	817 (5)	54 (5)	110 (3)
C(13)	3549 (5)	1531 (5)	816 (4)	109 (4)
C(14)	4579 (5)	2325 (4)	1127 (3)	89 (3)
Cl(3)	3333	6667	5149 (1)	129 (1)
C(15)	3333	6667	3752 (4)	72 (3)
C(16)	2214 (4)	5721 (3)	3415 (3)	71 (2)
C(17)	2133 (4)	5064 (4)	2609 (3)	81 (3)
C(18)	1115 (5)	4264 (4)	2251 (3)	96 (3)
C(19)	169 (5)	4094 (4)	2699 (5)	109 (3)
C(20)	222 (5)	4731 (5)	3497 (5)	115 (4)
C(21)	1237 (5)	5557 (4)	3858 (3)	100 (3)
H(3)	1319 (24)	2088 (24)	2215 (19)	95 (10)
H(4)	3084 (28)	3377 (28)	2784 (23)	129 (13)
H(5)	4080 (27)	2926 (28)	3982 (22)	128 (13)
H(6)	3131 (29)	1020 (29)	4689 (23)	139 (14)
H(7)	1321 (22)	−225 (22)	4140 (18)	83 (9)
H(10)	6072 (19)	1753 (19)	−380 (16)	56 (8)
H(11)	4341 (25)	375 (25)	−946 (20)	104 (11)
H(12)	2704 (28)	219 (28)	−199 (23)	127 (13)
H(13)	2925 (29)	1535 (30)	1156 (23)	140 (14)
H(14)	4700 (24)	2881 (22)	1680 (19)	89 (10)
H(17)	2836 (25)	5191 (25)	2262 (21)	103 (11)
H(18)	1092 (25)	3833 (26)	1614 (22)	112 (11)
H(19)	−517 (28)	3522 (29)	2419 (23)	129 (13)
H(20)	−386 (27)	4662 (29)	3872 (22)	128 (12)
H(21)	1318 (26)	6018 (24)	4435 (20)	104 (11)

Molecular geometry

The bond lengths and angles are given in Tables 2 and 3, respectively. Each of the three independent propeller-shaped TPCM molecules has its C—Cl bond coincident with a crystallographic threefold axis and therefore possesses C_3 symmetry. In the following, the salient features of the unique part of each independent molecule will be discussed and the listed quantities will

* Lists of structure factors and anisotropic thermal parameters have been deposited with the British Library Lending Division as Supplementary Publication No. SUP 36376 (13 pp.). Copies may be obtained through The Executive Secretary, International Union of Crystallography, 5 Abbey Square, Chester CH1 2HU, England.

Table 2. *Bond lengths* (Å) *with e.s.d.'s*

$\bar{d}$ is the weighted mean value calculated over the three molecules. σ'_m and σ_m are defined in the text ($\times 10^3$ for C–C, $\times 10^2$ for C–H bonds).

Molecule (I)		Molecule (II)		Molecule (III)		$\bar{d}$	σ'_m	σ_m
C(1)–Cl(1)	1·874 (6)	C(8)–Cl(2)	1·847 (6)	C(15)–Cl(3)	1·843 (6)	1·855	3	10
C(1)–C(2)	1·529 (4)	C(8)–C(9)	1·522 (4)	C(15)–C(16)	1·527 (4)	1·526	2	3
C(2)–C(3)	1·403 (7)	C(9)–C(14)	1·387 (8)	C(16)–C(21)	1·398 (9)	1·396	5	7
C(3)–C(4)	1·387 (7)	C(13)–C(14)	1·371 (8)	C(20)–C(21)	1·393 (7)	1·383	4	9
C(4)–C(5)	1·370 (10)	C(12)–C(13)	1·372 (9)	C(19)–C(20)	1·358 (9)	1·367	5	6
C(5)–C(6)	1·363 (8)	C(11)–C(12)	1·367 (10)	C(18)–C(19)	1·359 (10)	1·363	5	3
C(6)–C(7)	1·392 (6)	C(10)–C(11)	1·392 (7)	C(17)–C(18)	1·384 (6)	1·389	4	4
C(2)–C(7)	1·378 (7)	C(9)–C(10)	1·383 (7)	C(16)–C(17)	1·374 (7)	1·378	4	4
C(3)–H(3)	1·00 (4)	C(14)–H(14)	1·02 (3)	C(21)–H(21)	0·97 (3)	1·00	2	2
C(4)–H(4)	0·96 (4)	C(13)–H(13)	0·99 (4)	C(20)–H(20)	0·95 (4)	0·96	2	2
C(5)–H(5)	1·02 (3)	C(12)–H(12)	1·01 (3)	C(19)–H(19)	0·97 (3)	1·00	2	2
C(6)–H(6)	1·06 (4)	C(11)–H(11)	1·02 (3)	C(18)–H(18)	1·03 (2)	1·03	2	2
C(7)–H(7)	1·02 (3)	C(10)–H(10)	0·99 (3)	C(17)–H(17)	1·02 (4)	1·01	2	1

Table 3. *Bond angles* (°) *with e.s.d.'s*

$\bar{\theta}$ is the weighted mean value calculated over the three molecules (σ'_m and $\sigma_m \times 10$)

Molecule (I)		Molecule (II)		Molecule (III)		$\bar{\theta}$	σ'_m	σ_m
Cl(1)–C(1)–C(2)	106·2 (3)	Cl(2)–C(8)–C(9)	106·0 (3)	Cl(3)–C(15)–C(16)	107·0 (3)	106·4	1	3
C(2)–C(1)–C(2)	112·6 (3)	C(9)–C(8)–C(9)	112·7 (3)	C(16)–C(15)–C(16)	111·9 (3)	112·4	4	3
C(1)–C(2)–C(3)	120·6 (5)	C(8)–C(9)–C(14)	121·3 (4)	C(15)–C(16)–C(21)	121·1 (4)	121·0	2	3
C(1)–C(2)–C(7)	121·4 (4)	C(8)–C(9)–C(10)	121·2 (4)	C(15)–C(16)–C(17)	120·8 (4)	121·1	2	2
C(3)–C(2)–C(7)	118·0 (4)	C(10)–C(9)–C(14)	117·4 (4)	C(17)–C(16)–C(21)	117·9 (4)	117·8	2	3
C(2)–C(3)–C(4)	120·0 (6)	C(9)–C(14)–C(13)	121·6 (5)	C(16)–C(21)–C(20)	120·1 (5)	120·6	3	8
C(3)–C(4)–C(5)	121·0 (5)	C(12)–C(13)–C(14)	119·9 (6)	C(19)–C(20)–C(21)	120·6 (6)	120·6	3	5
C(4)–C(5)–C(6)	119·4 (4)	C(11)–C(12)–C(13)	120·3 (5)	C(18)–C(19)–C(20)	119·7 (5)	119·8	3	4
C(5)–C(6)–C(7)	120·5 (6)	C(10)–C(11)–C(12)	119·4 (5)	C(17)–C(18)–C(19)	120·8 (5)	120·2	3	6
C(2)–C(7)–C(6)	121·1 (4)	C(9)–C(10)–C(11)	121·3 (5)	C(16)–C(17)–C(18)	120·9 (5)	121·1	3	2
C(2)–C(3)–H(3)	117 (1)	C(9)–C(14)–H(14)	116 (2)	C(16)–C(21)–H(21)	116 (2)	116·4	10	6
C(4)–C(3)–H(3)	123 (2)	C(13)–C(14)–H(14)	123 (2)	C(20)–C(21)–H(21)	124 (2)	123·1	10	3
C(3)–C(4)–H(4)	115 (2)	C(14)–C(13)–H(13)	116 (2)	C(21)–C(20)–H(20)	114 (2)	114·7	11	10
C(5)–C(4)–H(4)	124 (2)	C(12)–C(13)–H(13)	124 (2)	C(19)–C(20)–H(20)	126 (2)	124·8	11	9
C(4)–C(5)–H(5)	118 (2)	C(13)–C(12)–H(12)	123 (2)	C(20)–C(19)–H(19)	123 (3)	121·2	14	22
C(6)–C(5)–H(5)	122 (2)	C(11)–C(12)–H(12)	117 (2)	C(18)–C(19)–H(19)	117 (3)	118·8	14	25
C(5)–C(6)–H(6)	124 (2)	C(12)–C(11)–H(11)	125 (2)	C(19)–C(18)–H(18)	121 (2)	123·1	10	15
C(7)–C(6)–H(6)	116 (2)	C(10)–C(11)–H(11)	116 (2)	C(17)–C(18)–H(18)	118 (2)	116·6	10	10
C(2)–C(7)–H(7)	120 (2)	C(9)–C(10)–H(10)	118 (1)	C(16)–C(17)–H(17)	119 (2)	118·7	8	5
C(6)–C(7)–H(7)	119 (2)	C(11)–C(10)–H(10)	120 (1)	C(18)–C(17)–H(17)	120 (2)	120·1	8	5

refer, in sequence, to the molecules (I), (II) and (III) respectively, as labelled in Fig. 1. Weighted mean values were calculated over equivalent bonds and angles. The associated e.s.d.'s, $\sigma_m = [\sum_i w_i(x_i - \bar{x}_m)^2/(N-1)\sum_i w_i]^{1/2}$ and $\sigma'_m = (\sum_i w_i)^{-1/2}$, where $w_i = \sigma_i^{-2}$, are, respectively, measures of the 'external' and 'internal' consistency (Domenicano, Vaciago & Coulson, 1975).

The C–Cl bond lengths, 1·874, 1·847 and 1·843 Å, are long when compared to the standard values 1·78–1·79 Å for C(sp^3)–Cl (Altona, Knobler & Romers, 1963). Long C–Cl distances have also been found in related compounds such as tris(*p*-methoxyphenyl)chloromethane, 1·860 (16) Å (Dunand & Gerdil, 1976*a*), and 2,3-dichloro-3,3-diphenylpropene-1,1-dicarbonitrile, 1·836 (2) Å (Schlodder & Ibers, 1975). A structural survey of the aliphatic chloro compounds clearly indicates that the C–Cl bond distances increase regularly with decreasing C–C–Cl angles (Dunand, 1977). The bond lengths range roughly from 1·70 to 1·88 Å whereas the bond angles decrease correspondingly from 125 to 104°. The geometries observed for the three TPCM molecules fit into this scheme. The distortion from tetrahedral angular symmetry at the central C_c atom results in the closure of the C_i–C_c–Cl angles to 106·2, 106·0 and 107·0° and in the concomitant expansion of the C–C_c–C angles to 112·6, 112·7 and 111·9° respectively. Almost identical angular parameters are found for the isostructural triphenylbromomethane (Dunand & Gerdil, 1981). Average C–C_c–Cl and C–C_c–C angle values of 106·2, 112·5° and 106·9, 111·8° are likewise observed for tris(*p*-methoxyphenyl)chloromethane and 2,3-dichloro-3,3-diphenylpropene-1,1-dicarbonitrile, respec-

tively. Interestingly, unsubstituted triphenylmethane undergoes the same angular distortion in its trigonal benzene solvate ($C-C_c-H$ = 106·6°, $C-C_c-C$ = 112·2°; Allemand & Gerdil, 1975) and in the orthorhombic unsolvated form (average $C-C_c-C$ = 112·6°; Riche & Pascard-Billy, 1974). This suggests that the internal $C-C_c-C$ angles are mainly controlled by the overall repulsion between the phenyl rings, while the torsion angles about C_i-C_c bonds are accommodated to the steric interaction with the apical atom. For the three conformations of TPCM these torsion angles are 50·7, 46·4 and 42·9°, respectively. The phenyl groups are slightly bent away from the Cl atom as expressed by the angles 3·1, 2·7 and 4·0° between the central bonds and their projection on the mean plane of the attached ring. The closer intramolecular $C_i\cdots C_{o,\mathbf{d}}$ contacts [2·863 (7), 2·868 (6), 2·855 (7) Å] are hardly longer than the distance separating two 'clamped' 1,4-carbon atoms of a benzene ring.

As expected the longer distances $C_i\cdots C_{o,\mathbf{p}}$ [3·150 (8), 3·271 (6), 3·336 (6) Å] and $C_{o,\mathbf{p}}\cdots C_{o,\mathbf{d}}$ [3·168 (8), 3·271 (6), 3·336 (6) Å] increase significantly with a decreasing twist about the central bond. In contrast the local variations of the $C_{o,\mathbf{p}}\cdots Cl$ [3·112 (5), 3·054 (5), 3·062 (6) Å] and $H_{o,\mathbf{p}}\cdots Cl$ [2·80 (3), 2·68 (3), 2·67 (3) Å] separations are the results of more intricate steric interferences.

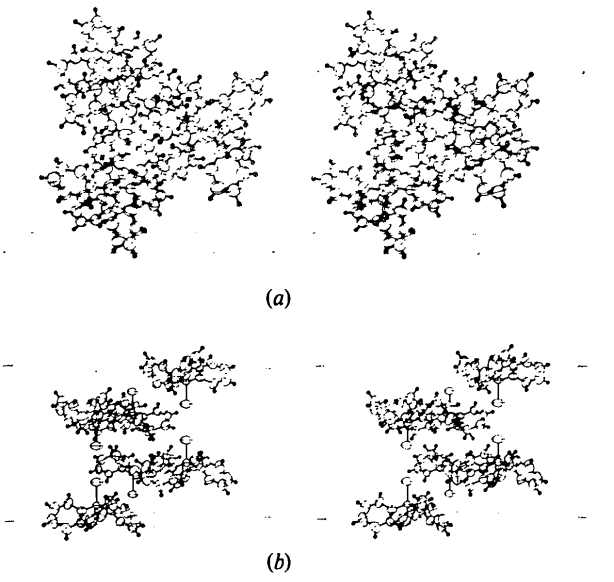

Fig. 2. Stereoscopic views of the unit-cell contents (*a*) down the *c* axis with the origin in the rear upper left corner; (*b*) with the *c* axis pointing upward, and the origin located in the rear lower corner (the chain-dotted lines represent the crystallographic threefold axes). The vibrational ellipsoids of the non-hydrogen atoms are plotted at the 50% probability level; the H atoms were given an arbitrary 0·1 Å radius.

Crystal packing analysis

Owing to the TPCM molecules being positioned on the crystallographic threefold axes the molecular packing can be described in terms of two distinct head-to-head arrangements of pairs of molecules (see Fig. 2). Molecule (I) lies on the rotatory-inversion axis and is coupled with its enantiomer (I′). The molecular pair (II)–(III′), and its equivalent (II′)–(III), are located on the proper threefold axes, and have their components interrelated by 'pseudo' symmetry centres at about $\frac{2}{3},\frac{1}{3},\frac{4}{11}$ and $\frac{1}{3},\frac{2}{3},\frac{7}{11}$ respectively. In the first $C-Cl\cdots Cl'-C'$ collinear arrangement, the halogen separation $Cl(1)\cdots Cl'(1)$ is 3·583 (3) Å, a value consistent with the sum of the van der Waals radii as proposed by Bondi (1964). The other contact $Cl(2)\cdots Cl'(3)$ = 3·210 (3) Å is even shorter than the separation of 3·34 Å that would be exhibited by two non-bonded non-spherical Cl atoms flattened at their poles (Collin, 1956; Nyburg, 1979). Intermolecular $C\cdots H$ and $H\cdots H$ contacts behave normally [shortest contacts: $C\cdots H$ = 2·84 (3); $H\cdots H$ = 2·38–2·52 Å].

A minimization of the crystal lattice energy with respect to the lattice constants, molecular translations and rotations was performed by means of the *PCK*6 program (Williams, 1972, 1974). The X-ray structures of the TPCM molecules were retained throughout the calculations. For the purpose of comparison two sets of values were used as adjustable parameters in the function $U(r) = -Ar^{-6} + B\exp(-Cr)$ representing the non-bonded interatomic potential energy. The first set (hereafter W–BB) included the values as fitted by Williams (1974) for $C\cdots C$ and $C\cdots H$ interactions and those of Bates & Busing (1974) for the $Cl\cdots Cl$ interactions. For the mixed interactions, the geometric mean combining law was assumed for the A and B coefficients and the arithmetic mean for the C coefficient. The second set (hereafter MC) consisted of the coefficients derived by Mirsky & Cohen (1978).

The effects of including electrostatic charges on the atoms were evaluated with both sets of parameters. Point charges were calculated by the EHT method (Hoffmann, 1963) for a fixed geometry arbitrarily taken as that of molecule (I), and using the parameterization of Jordan (1968). The point charges are: Cl, −0·28; C(1), +0·33; C(2), +0·08 e; the charge separations range from 0·22 to 0·32 e on the C–H bonds as compared with the values 0·358–0·414 e derived from lattice-energy calculations for a set of aromatic and saturated hydrocarbons (Williams, 1974). The calculated dipole moment μ_c = 7·47 × 10^{-30} Cm is in good agreement with the observed one, μ_e = 6·67 × 10^{-30} Cm (McClellan, 1963). All the lattice sums were evaluated with convergence acceleration (Williams, 1971). The convergence constants $K = K_6 = K_1$ were 0·150 in both the dispersion and Coulombic terms. The K value corresponds to a shallow minimum of the function of the minimized

Table 4. *Molecular packing analysis*

Potential field	W–BB		MC	
Lattice energy (kJ mol^{-1})	−264·4	−166·1*	−364·8	−276·6*
Calculated a (Å)	13·756	13·699	13·443	13·388
Calculated c (Å)	13·309	13·277	12·815	12·772
Cl(1)···Cl′(1) (Å)	3·637	3·644	3·352	3·358
Attractive term (kJ mol^{-1})	−1·6	−1·6	−4·4	−4·4
Repulsive term (kJ mol^{-1})	1·3	1·3	4·9	4·8
Coulombic term (kJ mol^{-1})	–	14·6	–	15·9
Non-bonding potential (kJ mol^{-1})	−0·3	14·3	0·5	16·4
Cl(2)···Cl′(3) (Å)	3·409	3·414	3·166	3·158
Attractive term (kJ mol^{-1})	−4·6	−4·6	−12·4	−12·6
Repulsive term (kJ mol^{-1})	5·6	5·6	14·9	15·1
Coulombic term (kJ mol^{-1})	–	31·2	–	33·8
Non-bonding potential (kJ mol^{-1})	1·0	32·2	2·5	36·3

* Including Coulombic interactions.

Table 5. *Rigid-body-motion analysis*

Shown are eigenvalues of the **L** and **T** tensors referred to a Cartesian coordinate system with z coaxial with the molecular C_3 axis. The **T** components are given in their reduced form (Schomaker & Trueblood, 1968).

Molecule	(I)	(II)	(III)
L_{11}* (deg^2)	14·0 (6)	21·1 (7)	22·9 (1·0)
L_{33}	7·1 (1·2)	4·6 (1·5)	2·2 (1·9)
T_{11} (Å^2)	0·075 (2)	0·078 (2)	0·080 (2)
T_{33}	0·050 (1)	0·043 (1)	0·042 (2)
$\langle \Delta^2 U_{ij} \rangle^{1/2}$	0·0048	0·0057	0·0076
$\langle \sigma^2 U_{ij} \rangle^{1/2}$	0·0033	0·0034	0·0035
$\langle \Delta^2 U_{ij}(\mathrm{Cl}) \rangle^{1/2}$	0·0018	0·0027	0·0040
$\langle \Delta^2 U_{ij}(\mathrm{C}_c) \rangle^{1/2}$	0·0045	0·0082	0·0101
R†	0·088	0·087	0·123

* $L_{11} = L_{12}$; $T_{11} = T_{12}$.
† $R = \sum w|\Delta U_{ij}| / \sum w|U_{ij}|$.

lattice energy *versus* K, the electrostatic contribution being omitted. The direct lattice sum was *truncated selectively* for each type of atom···atom interaction, that is for large interatomic distances at which the interaction energy became smaller than −0·002 kJ mol^{-1}. Thermal effects were not taken into account. Representative energy results are given in Table 4. The major difference between the two sets of potential functions lies in the Cl···Cl interactions, which appear to be 'harder' when described with the Bates–Busing potentials. With the latter both unique Cl···Cl distances are calculated longer than those observed at room temperature, whereas the reverse situation arises with the Mirsky–Cohen potentials. In both instances, however, the unusually close Cl(2)···Cl′(3) contact is calculated shorter than the separation at which the potential energy is zero. Thus the present crystal packing models are consistent with a net repulsion arising between the halogen atoms (see below). In addition, the observed shortening of the C–Cl(2) and C–Cl(3) bonds relative to C–Cl(1) might be a direct consequence of the steric compression occurring along the bond axis direction.

Thermal-motion analysis

The Cl atoms display a strongly anisotropic thermal motion with a large component normal to the threefold molecular axis. The r.m.s. displacements normal to and along the axis direction are, respectively, 0·376 and 0·227 Å for Cl(1), 0·385 and 0·210 Å for Cl(2), and 0·415 and 0·209 Å for Cl(3) (m.s.d. 0·002 Å). The displacement component of the central C atom along the threefold-axis direction is approximately equal to that of the Cl atom to which it is bonded. Its component normal to the axis, averaged over the three TPCM molecules, is 0·29 Å.

The thermal motion associated with the C–Cl bonds could be mistaken for some kind of disorder whereby the bonds would be tilted away from the threefold axis in order to reduce the repulsive interaction inherent in a linear head-to-head arrangement. This situation, however, appears unlikely in view of the following facts. First a ΔF synthesis shows no unusual features around the Cl atoms. Second the results of the rigid-body-motion analysis carried out with the *THMB* program (Trueblood, 1978) indicate, for each independent molecule, that the thermal motion of the C–Cl group is not dissociated from that of the whole molecule. This is evidenced, in particular, by the fair agreement between the observed and calculated U_{ij}'s for the Cl and C_c atoms and, as a whole, by the satisfactory R values (Table 5). For molecules (I), (II) and (III), the thermal motion is described in a coordinate system in which the libration axes intersect on the C_3 molecular axis, in the central region of the molecule, respectively at distances 2·004, 1·381 and 1·677 Å from the C_c atom. It can further be calculated from the magnitude of the relevant tensors elements that the large motional displacement of the Cl atom perpendicular to the C_3 axis is due to translation and libration in approximately equal proportions.

Discussion

The question might be raised as to whether partial intermolecular bonding contributes to the occurrence of the present short Cl···Cl contacts. This possibility had been suggested by Stora (1953) in an early report on the isomorphous triphenylbromomethane. In such an event, electron transfer towards the intermolecular 'bonding region' would also favour the lengthening of the adjoining carbon–halogen bonds. Intermolecular bonding has been put forward to account for unusually short non-bonded halogen···halogen separations in the crystal structures of chlorine (Hillier & Rice, 1967) and

of the haloforms (Kawaguchi, Takashina, Tanaka & Watanabé, 1972). However, the matter cannot be disputed in the present study where no separate estimation is made of the contribution of the exchange energy term of the repulsive potentials. Despite that, a satisfactory picture of the packing forces emerges from the present mechanical models and no additional assumptions seem required to explain the striking features of the crystal packing. Moreover, as is stressed above, the respective magnitudes of the internal molecular parameters lie within the expected ranges.

References

ALLEMAND, J. & GERDIL, R. (1975). *Acta Cryst.* A**31**, S130.

ALTONA, C., KNOBLER, C. & ROMERS, C. (1963). *Acta Cryst.* **16**, 1217–1225.

BATES, J. B. & BUSING, W. R. (1974). *J. Chem. Phys.* **60**, 2414–2419.

BONDI, A. (1964). *J. Phys. Chem.* **68**, 441–451.

COLLIN, R. L. (1956). *Acta Cryst.* **9**, 537.

DOMENICANO, A., VACIAGO, A. & COULSON, C. A. (1975). *Acta Cyst.* B**31**, 221–234.

DUNAND, A. (1977). Thesis n° 1778, Univ. de Genève.

DUNAND, A. & GERDIL, R. (1976*a*). *Acta Cryst.* B**32**, 1591–1593.

DUNAND, A. & GERDIL, R. (1976*b*). *Z. Kristallogr.* **144**, 419.

DUNAND, A. & GERDIL, R. (1981). In preparation.

GERDIL, R. & DUNAND, A. (1975). *Acta Cryst.* B**31**, 936–937.

GOMBERG, M. (1900). *Chem. Ber.* **33**, 3150–3163.

HEMILIAN, W. (1874). *Chem. Ber.* **7**, 1203–1210.

HILLIER, I. H & RICE, S. A. (1967). *J. Chem. Phys.* **46**, 3881–3889.

HOFFMANN, R. (1963). *J. Chem. Phys.* **39**, 1397–1412.

JORDAN, F. (1968). *Theoret. Chim. Acta*, **11**, 390–400.

KAWAGUCHI, T., TAKASHINA, K., TANAKA, T. & WATANABÉ, T. (1972). *Acta Cryst.* B**28**, 967–972.

LANDAIS, J. (1953). *Bull. Soc. Chim. Fr.* pp. 648–655.

MCLELLAN, A. L. (1963). *Tables of Experimental Dipole Moments*. San Francisco: Freeman.

MIRSKY, K. & COHEN, M. D. (1978). *Chem. Phys.* **28**, 193–204.

NYBURG, S. C. (1979). *Acta Cryst.* A**35**, 641–645.

RICHE, C. & PASCARD-BILLY, C. (1974). *Acta Cryst.* B**30**, 1874–1876.

SCHLODDER, R. & IBERS, J. A. (1975). *Acta Cryst.* B**31**, 708–712.

SCHOMAKER, V. & TRUEBLOOD, K. N. (1968). *Acta Cryst.* B**24**, 63–76.

STORA, C. (1953). *Bull. Soc. Chim. Fr.* pp. 1059–1063.

STORA, C. & POYER, N. (1966). *Bull. Soc. Chim. Fr.* pp. 841–849.

TRUEBLOOD, K. N. (1978). *Acta Cryst.* A**34**, 950–954.

WANG, S.-N. & LU, C.-S., (1944). *J. Am. Chem. Soc.* **66**, 1113–1114.

WILLIAMS, D. E. (1971). *Acta Cryst.* A**27**, 452–455.

WILLIAMS, D. E. (1972). *Acta Cryst.* A**28**, 629–635.

WILLIAMS, D. E. (1974). *Acta Cryst.* A**30**, 71–77.

XRAY system (1972). Version of June 1972. Tech. Rep. TR-192, Computer Science Center, Univ. of Maryland, College Park, Maryland.

YOUNG, J. (1931). BS thesis, Massachusetts Institute of Technology, unpublished. Cited in A. N. WINCHELL (1954), *The Optical Properties of Organic Compounds*, New York: Academic Press.

Acta Cryst. (1982). B**38**, 575–580

The Structure of 9-[3-(3-Indolyl)propyl]adenine. A Model for Protein/Nucleic Acid Interactions*

BY GERARD BUNICK† AND DONALD VOET

Department of Chemistry, University of Pennsylvania, Philadelphia, Pennsylvania 19104, *USA*

(*Received* 17 *March* 1981; *accepted* 6 *August* 1981)

Abstract

The X-ray crystal structure of 9-[3-(3-indolyl)propyl]-adenine [$C_{16}H_{16}N_6$, space group $P2_1/n$, $Z = 4$, $a = 14{\cdot}751\ (4)$, $b = 8{\cdot}239\ (2)$, $c = 12{\cdot}160\ (2)$ Å, $\beta = 97{\cdot}94\ (3)°$, $V = 1463{\cdot}7$ Å^3, $D_c = 1{\cdot}339$ Mg m^{-3}] has been solved and refined to a final R factor of 0·073 based on 1469 observed reflections. This molecule, which serves as a model for protein/nucleic acid associations, crystallizes in an extended conformation. The adenine residues in the structure form endless hydrogen-bonded chains. However, the indole and adenine groups are out of contact with one another. A similar lack of indole/adenine associations is observed in the two other known crystal structures containing

* Research supported by National Institutes of Health Grant GM23966.

† Present address: University of Tennessee, Chemistry Division, PO Box X, Oak Ridge National Laboratory, Oak Ridge, Tennessee 37830, USA.

0567-7408/82/020575-06$01.00

© 1982 International Union of Crystallography